

Over 100nm Wavelength Conversion Bandwidth with High Efficiency on AlGaAsOI Nonlinear Waveguides

Zhengshun Lei¹, Weiqiang Xie^{1,*}, Wenqi Wei², Zihao Wang², Ting Wang², Jianjun Zhang², and Yikai Su¹

¹State Key Lab of Advanced Optical Communication Systems and Networks,

Department of Electronic Engineering, Shanghai Jiao Tong University, Shanghai 200240, China

²Beijing National Laboratory for Condensed Matter Physics, Institute of Physics, Chinese Academy of Sciences, Beijing 100190, China

*weiqiang.xie@sjtu.edu.cn

Abstract: A nonlinear wavelength conversion with over 100nm bandwidth and >−10dB conversion efficiency on AlGaAsOI waveguides is demonstrated, using a low-power and single continuous-wave pump. Theoretical simulations are in excellent agreement with the experimental results. © 2024 The Author(s)

OCIS codes: (130.0130) Integrated optics, (190.0190) Nonlinear optics

1. Introduction

Nonlinear wavelength conversion based on four-wave mixing (FWM) has a wide range of applications in optical signal processing, such as optical communications and quantum metrology. Traditional wavelength conversion using fiber-based systems requires large pump powers and a long effective length to increase bandwidth and conversion efficiency (CE). Consequently, integrated photonics using nanowaveguides, due to their tight mode confinement and large nonlinearity, are considered potential solutions to achieve low-power on-chip wavelength conversions with large bandwidth. In fact, high-confinement silicon waveguides based on silicon-on-insulator platform have been used to demonstrate nonlinear wavelength conversion [1]. However, Si waveguides suffer from inevitable nonlinear losses such as two-photon absorption and related free-carrier losses at telecommunication wavelengths. Other platforms with lower nonlinear losses such as silicon nitride (Si₃N₄) and aluminum gallium arsenide (AlGaAs) have also been investigated. For example, low-loss, meter-scale-long, high-confinement dispersion-engineered Si₃N₄ spiral waveguides have been utilized to perform the FWM process with a conversion bandwidth of less than 40 nm, using an input power of over 2 W at a continuous-wave (CW) pump [2].

Compared to Si₃N₄, AlGaAs offers even stronger nonlinearity ($n_2 \approx 2.6 \times 10^{-17} m^2 W^{-1}$) and a higher linear refractive index close to Si, leading to a huge nonlinear waveguide parameter (γ). In particular, the recent development of low-loss and high-confinement AlGaAs waveguides based on AlGaAs-on-insulator (AlGaAsOI) platform has triggered various on-chip, high-efficiency nonlinear applications [3-7]. Consequently, the potential capability of wide-bandwidth and high CE nonlinear wavelength conversions using AlGaAs nanowaveguides becomes attractive, yet remains unexplored. In this work, we develop low-loss (<0.4 dB/cm) AlGaAs spiral waveguides with cm-scale lengths and use a single CW pump for nonlinear wavelength conversion. An over 100 nm conversion bandwidth with a flat CE of >−10 dB is demonstrated at pump powers less than 100 mW. Notably, the length of AlGaAs waveguide is only 3 cm for such high-performance wavelength conversion. A theoretical modeling is also presented, showing an excellent agreement with the experimental results. Our results highlight the great potential of AlGaAs in enabling efficient and high-bandwidth wavelength conversion as well as other on-chip nonlinear applications and thus open up new avenues for achieving compact and high-performance nonlinear photonic functionalities.

2. Propagation Principle

Using the basic propagation equation [8], the propagation of the optical field along AlGaAs waveguides can be expressed by the nonlinear Schrödinger equation (NLSE),

$$\frac{dA_p}{dz} = \left[i\gamma \left(|A_p|^2 + 2|A_s|^2 + 2|A_i|^2 \right) - \frac{\alpha}{2} \right] A_p + i\gamma A_p^* A_s A_i \cdot e^{i\Delta\beta z}, \quad (1)$$

$$\frac{dA_s}{dz} = \left[i\gamma \left(2|A_p|^2 + |A_s|^2 + 2|A_i|^2 \right) - \frac{\alpha}{2} \right] A_s + i\gamma A_p^2 A_i^* \cdot e^{-i\Delta\beta z}, \quad (2)$$

$$\frac{dA_i}{dz} = \left[i\gamma \left(2|A_p|^2 + 2|A_s|^2 + |A_i|^2 \right) - \frac{\alpha}{2} \right] A_i + i\gamma A_p^2 A_s^* \cdot e^{-i\Delta\beta z}, \quad (3)$$

where A_p, A_s, A_i represent the normalized slowly varying envelope of the optical field along propagation distance z for pump, signal and idler, respectively. α denotes the linear waveguide propagation loss. The nonlinear waveguide parameter is defined as $\gamma = 2\pi n_2/\lambda A_{\text{eff}}$, in which λ is the pump wavelength and A_{eff} is the all-vectorial effective mode area for the waveguides of different widths [9]. The phase mismatch for FWM can be written as

$$\Delta\beta = 2\beta_p - \beta_i - \beta_s, \quad (4)$$

where $\beta_p, \beta_i, \beta_s$ are the propagation constant of the pump, signal and idler, respectively. The propagation equations are integrated using a four-order Runge-Kutta along z . The CE is defined by the ratio of the output idler power and the signal power without the pump. To maintain a large wavelength conversion bandwidth needs to minimize the phase mismatch, which means that the pump wavelength should be close to the regime of zero-dispersion. This can be readily realized via dispersion engineering by tailoring the dimension of AlGaAs nanowaveguides.

3. AlGaAs Waveguides and Experimental Results

The low-loss AlGaAsOI spiral waveguides were fabricated by using a heterogeneous wafer-bonding approach [5]. The fabrication process was optimized for a high device yield especially for cm-long waveguides without defects. The fabricated waveguides have a thickness of $\sim 350\text{nm}$ and various widths for dispersion adjustment. From numerical simulation, the widths in a range of 500 nm to 850 nm can cover the group-velocity dispersion (GVD) from anomalous to normal regimes around 1550 nm for fundamental transverse-electric (TE) mode. Figure 1(a) shows the scanning electron microscope (SEM) image of the cross section of the fabricated AlGaAs waveguide, indicating an almost perfect vertical sidewall. Figure 1(b) shows a 3-cm long spiral waveguide. The experimental setup for FWM wavelength conversion is shown in Figure 1(c). The pump and signal are output from two tunable lasers. An Erbium-doped fiber amplifier (EDFA) is used to amplify the pump. The pump and signal are controlled by two polarization controllers to maintain TE input to the waveguide, and then, combined using a 90/10 directional fiber coupler before entering the device under test (DUT). Optical spectrum analysis (OSA) and power meter (PM) are used to record the output spectra and the total output power, respectively. In our experiment, a 1550nm wavelength pump is used. The input signal is swept from 1480 nm to 1640 nm. We use the lensed fiber for coupling in/out to the waveguide. The edge coupler of the AlGaAs waveguide is carefully designed to achieve a coupling loss of about 3 dB/facet in the experiment.

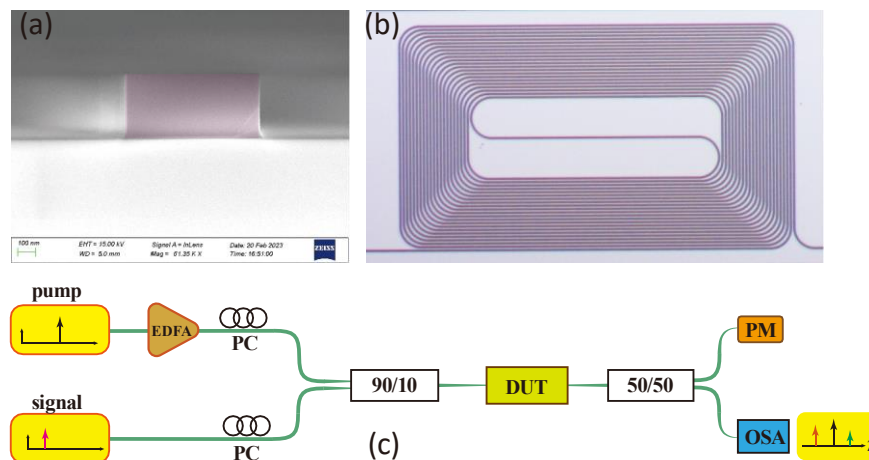


Fig. 1. (a) False-colored SEM image of AlGaAs waveguide cross section prior to oxide cladding. The waveguide has a dimension of $\sim 350\text{ nm} \times 700\text{ nm}$. (b) Optical microscope image of a 3-cm long AlGaAs waveguide. (c) The experimental setup for FWM wavelength conversion.

The wavelength conversion experiment of AlGaAs waveguides was conducted by using different on-chip pump power while maintaining an input signal power of 0 dBm. Figure 2 shows the experimental results for the waveguide which has a length of 3 cm and a cross-sectional dimension of $\sim 350\text{ nm} \times 700\text{ nm}$. Figure 2(a) shows the CE spectrum in a wavelength range of 1480nm to 1640nm at an on-chip pump power of $\sim 14\text{ dBm}$. At a higher pump power of $\sim 17\text{ dBm}$, a conversion bandwidth is over 70 nm with a flat CE of -10 dB , as shown in Figure 2(b). As increasing the pump power, the conversion bandwidth further increases. At a pump power of $\sim 20\text{ dBm}$, a conversion bandwidth from 1493nm to 1612nm with a CE $> -10\text{ dB}$ can be achieved together with excellent flatness. The average CE is about -4

dB over a conversion bandwidth of more than 100 nm. An average CE of ~ 0 dB can be reached when the pump power is increased to 23dBm, as shown in Figure 2(d). Furthermore, theoretical simulations (blue solid lines in Figure 2) were also performed using Eq (1) to (3). Here, we implement the all-vector coupled mode theory to obtain a more accurate A_{eff} of AlGaAs waveguide in the theoretical simulation for CE spectrum, and the results are in excellent agreement with the experimental data as shown in Figure 2. Besides, it should be mentioned that the presence of the fluctuation in CE at different wavelengths could be attributed to the mode conversion and interference between fundamental TE mode and high-order modes at bending regions of the spiral waveguide. This can be improved by a careful bending design for a smooth transition of the fundamental TE mode. In the experiment, we also performed tests on waveguides with varying lengths and widths ranging from 500 nm to 850 nm, and found that the waveguide with a width of around 700nm gives the optimal conversion performance in terms of bandwidth, CE, and spectrum flatness. This can be explained by the fact that the numerically calculated GVD for widths around 700nm is close to zero at 1550nm, thus resulting in a minimized phase mismatch for nonlinear wavelength conversion.

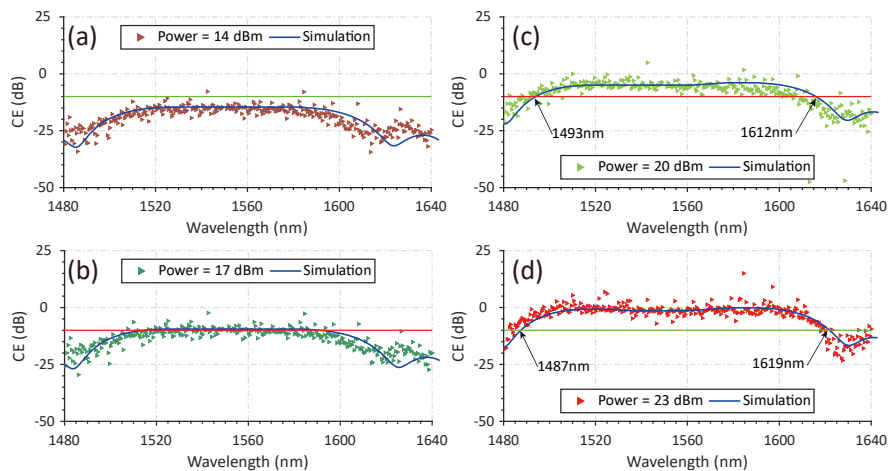


Fig. 2. The spectra of on-chip CE for different pump power. The blue line is simulated CE. The on-chip input pump powers in (a-d) are 14 dBm, 17dBm, 20dBm, and 23dBm, respectively.

4. Conclusions

In summary, we have experimentally demonstrated a CW-pumped wavelength conversion in low-loss AlGaAs spiral waveguides at the telecommunication bands. A conversion bandwidth of over 100 nm with a high and flat CE (> -10 dB) is observed with less than 100 mW input pump powers. These findings provide further insights into the wavelength conversion capabilities of highly nonlinear AlGaAs waveguides. With the advantages of large CE bandwidth and low pump power, AlGaAs waveguides may have great potential for on-chip signal nonlinear processing in optical communications and quantum optics.

Acknowledgments

This work was supported by the National Natural Science Foundation of China (Grant No. 62175149) and the National Key Research and Development Program of China (2021YFB2800603). The work was also sponsored by the Shanghai Pujiang Program and the National Science Fund Program for Distinguished Young Scholars (Overseas).

References

- [1] M. A. Foster, et al., "Broad-band optical parametric gain on a silicon photonic chip." *Nat.* **441**, 960-963 (2006).
- [2] Z. Ye, et al., "Overcoming the quantum limit of optical amplification in monolithic waveguides." *Sci. Adv.* **7**, eabi8150 (2021).
- [3] M. Pu, et al., "Efficient frequency comb generation in AlGaAs-on-insulator." *Optica* **3**, 823-826 (2016).
- [4] L. Chang, et al., "Ultra-efficient frequency comb generation in AlGaAs-on-insulator microresonators." *Nat. Commun.* **11**, 1331 (2020).
- [5] W. Xie, et al., "Ultra-high-Q AlGaAs-on-insulator microresonators for integrated nonlinear photonics." *Opt. Express* **28**, 32894-32906 (2020).
- [6] M. Pu, et al., "Ultra-Efficient and broadband nonlinear AlGaAs-on-insulator chip for low-power optical signal processing." *Laser Photonics Rev.* **12**, 1800111 (2018).
- [7] J. Qin, et al., "On-chip high-efficiency wavelength multicasting of PAM3/PAM4 signals using low-loss AlGaAs-on-insulator nanowaveguides." *Opt. Lett.* **45**, 4539-4542 (2020).
- [8] G. Agrawal, *Nonlinear Fiber Optics* (Academic Press, ed. 5, 2013), Chap 3.
- [9] K. Guo, et al., "Full-vectorial propagation model and modified effective mode area of four-wave mixing in straight waveguides." *Opt. Lett.* **42**, 3670-3673 (2017).